Thermochimica Acta 618 (2015) 36–47

Contents lists available at ScienceDirect

Thermochimica Acta

journal homepage: www.elsevier.com/locate/tca

Synergism among biomass building blocks? Evolved gas and kinetics analysis of starch and cellulose co-pyrolysis

Junjie Xue[a,b], Selim Ceylan[c], Jillian L. Goldfarb[a,d,*]

[a] Department of Mechanical Engineering, Boston University, 110 Cummington Mall, Boston, MA 02215, United States
[b] College of Engineering, China Agricultural University, Beijing 100083, People's Republic of China
[c] Ondokuz Mayıs University, Faculty of Engineering, Chemical Engineering Department, 55139 Kurupelit, Samsun, Turkey
[d] Division of Materials Science and Engineering, Boston University, 15 St. Mary's Street, Brookline, MA 02446, United States

ARTICLE INFO

Article history:
Received 19 June 2015
Received in revised form 31 August 2015
Accepted 2 September 2015
Available online 6 September 2015

Keywords:
Pyrolysis
Biomass
Cellulose
Starch
Synergy
Evolved gas
Activation energy
Distributed activation energy model

ABSTRACT

Debate surrounds biomass co-pyrolysis: can thermal decomposition be modeled as the sum of individual components, or do synergistic reactions promote or hinder devolatilization? Activation energies of mixtures of starch and cellulose pyrolyzed at 10, 50 and 100 K/min were determined via the distributed activation energy model. Reaction kinetics suggest that blending may promote devolatilization, seen through lower activation energies. Yet, evolved gas analysis shows no evidence of synergism as a result of blending, at least at lower temperatures. As the percentage of cellulose increases, the temperature at which the peak mass loss rate occurs and peak evolved gases emerge are linearly related. As such, there is little evidence of chemical reaction synergism during the pyrolysis of these two biomass building blocks, but rather synergistic behavior is perhaps a result of the starch physically promoting the devolatilization of cellulose at lower temperatures when present in larger quantities.

1. Introduction

The 2007 United States Independence and Security Act mandates that 16 billion gallons of cellulosic biofuel be blended into traditional transportation fuels by 2022, a portion of which must be biodiesel produced from biomass [1]. The widespread use of biomass as a renewable feedstock for the production of liquid fuels and syngas depends on several factors. For the pyrolytic conversion of solids, these include the ability to design appropriate reaction systems, insure adequate supplies of feedstocks, standardize biomass-derived pyrolysis liquid products and, perhaps most importantly, develop a comprehensive understanding of the thermochemical pathways underlying the decomposition of solid biomass to liquid and gaseous fuels [2]. The ability to predict the behavior of mixed biomass streams during co-pyrolysis is imperative to insuring successful large-scale implementation of thermochemical conversion of biomass to biofuels.

A number of studies demonstrate the ability to alter bio-oil and pyrolysis gas composition and yield from pyrolysis, the thermal decomposition in the absence of oxygen, by changing reaction temperatures, pressures and heating rates [3,4] as well as exploiting reaction synergy among solid fuels to tailor the properties of the pyrolysis products by co-pyrolyzing biomasses [5]. This is critically important as we move forward with industrial scale production of bio-oils via thermal treatment. However, we require a deeper understanding as to the nature of these synergistic reactions. For example, does the physical compilation of solid fuels that devolatilize at lower temperatures than others cause changes in overall reaction rates and kinetics? Does blending fuel streams change the pyrolysis gas compositions evolving from solid blend pyrolysis? Can we predict the activation energies required to pyrolyze blended fuel streams from knowledge of their pure component characteristics, or does synergy impact activation energies? These and other questions must be answered on a fundamental level to better design industrial pyrolysis units and determine optimal feedstock blends. For that reason, here we investigate the kinetics and evolving gas compositions of two fundamental biomass building blocks with the same chemical formula but different molecular geometry: starch and cellulose.

* Corresponding author at: Department of Mechanical Engineering, Boston University, 110 Cummington Mall, Boston, MA 02215, United States.
E-mail addresses: JillianLGoldfarb@gmail.com, jilliang@bu.edu (J.L. Goldfarb).

http://dx.doi.org/10.1016/j.tca.2015.09.002
0040-6031/

There is discord in the literature about the nature of blended solid fuel pyrolysis; some find that the yields and activation energies of co-pyrolyzed fuels are linearly proportional to the contributions of the individual components [6,7]. Others detect non-additive compositions and activation energies across heating rates and temperature ranges [8–10]. And yet still others, our group included, find both additive and synergistic behavior for the same samples, such as the peak mass loss reaction rates found via derivative thermogravimetric curves displaying additive behavior (linearly increasing reaction rate as biomass percentage in coal–biomass blends increases) whereas the activation energy and evolved gas compounds of the same blends may display synergistic behavior [11,12]. However, there is scant information in the literature concerning whether varying the composition of blends can induce reaction synergism. A survey of singular source biomass components (i.e. feed corn stover, nut shells, wood samples) indicates that this would be the case; each of these biomasses is comprised of different ratios of cellulose, hemicellulose, lignin, starch, proteins, etc., and each displays a different thermal decomposition profile. Despite this accepted generalizability, the specific contribution of different biomass constituents to the overall kinetic behavior has yet to be explored.

Cellulose and starch are polymers of glucose, and represent the carbohydrate building blocks of biomass [13]. They have the same unit molecular formula $[C_6H_{10}O_5]_n$, though different molecular orientations. Starch is comprised of repeating glucose units oriented in the same direction (alpha linkages), whereas in cellulose, neighboring units are rotated 180° around the axis of the polymer chain backbone (beta linkages). The hydroxyl group attached to carbon-1 is below the plane of the ring in starch, and above for cellulose. Hydrogen bonding in the β-linked polymer is what lends cellulose its structural advantage, yielding a strong, fibrous nature, as compared to starch, which solubilizes fairly easily in water. There are a number of studies in the literature that describe the thermal decomposition of pure starch [14–16] and pure cellulose [17]; we could not locate any that probe the potential synergistic relationship that occurs among blends of these compounds. Starch and cellulose are a model system to probe the potential synergism between biomass constituents; they have the same composition but vastly different structural characteristics and known decomposition profiles. They are both known to thermally decompose via a dehydration → depolymerization → devolatilization pathway, but these reactions occur at different temperatures and rates for each material [15,17]. As such, we query whether or not the decomposition of starch can synergistically impact the onset of cellulose decomposition. That is, if we note synergism between these two components, then the starch may promote decomposition of the hydrogen-bonded cellulose, which would indicate the possibility of producing pyrolysis bio-oil and syngas at lower temperatures by blending biomass materials with lower energy barriers to decomposition in the overall raw material mixture. However, the results presented herein apply beyond bio-fuel production; as we seek new sources of renewable materials such as thermoplastics and biopolymers, knowledge of how blended biomass building blocks such as starch and cellulose behave under various thermal environments may assist in renewable materials design [18–22].

2. Materials and methods

2.1. Materials

Microcrystalline Cellulose (CAS: 9004-34-6) was purchased from Fisher Scientific, supplied by Alfa Aesar, Lot #10179415. Soluble Starch (CAS: 9005-84-9) was supplied by Fisher Scientific, Lot #136971 as Certified ACS Regent Grade. Samples were used as received. Approximately 1 g of each mixture was fabricated by weighing the desired amount of cellulose and starch on a Sartorius semi-microbalance to ±0.1 mg and placed into a clean glass vial, as given in Table 1. Contents were homogenized by placing the vials on a vortex mixer for several minutes. Samples were stored at ambient conditions until used.

Table 1
Mixtures of starch and cellulose used in pyrolysis experiments.

Sample	Cellulose	Starch	Mixture 1	Mixture 2	Mixture 3
Cellulose mass fraction	1.0	0	0.75	0.50	0.25
Starch mass fraction	0	1.0	0.25	0.50	0.75

2.2. Thermogravimetric analysis-differential scanning calorimetry (TGA–DSC)

Each pure solid fuel and blend was pyrolyzed in a high purity nitrogen atmosphere (reactive + protective gas flow at 70 mL/min) in a 70 μL alumina crucible using a Mettler Toledo TGA/DSC1 with gas flow control, data output to the Mettler STARe Default DB V10.00 software. The DSC was calibrated with indium standard (Mettler Toledo) at 10 K/min. The mass is measured every second to the 10^{-9} g, along with temperature to ±0.1 K. All samples were heated to 383 K and held for 15 min to insure moisture removal. Then the sample was heated at 10, 50 or 100 K/min up to 1173 K and held for 30 min to obtain a stable mass reading. Every sample was run at 10 K/min three times to insure reproducibility; each sample at 50 K and 100 K/min was run once, with random samples run a second and third time to insure reproducibility.

There are multiple methods available to analyze the pyrolysis kinetics of solid carbonaceous fuels. Many are based off of the Arrhenius equation, expressed in the general form as:

$$k = Ae^{-E/RT} \tag{1}$$

where A is the frequency (or pre-exponential) factor, E the activation energy, T the absolute temperature, R the universal gas constant, and k is the reaction rate constant. It is often assumed that the thermal decomposition of carbonaceous fuels such as biomass occurs as an infinitely large set of first order reactions, allowing for the calculation of an overall, or apparent activation energy assuming an overall, or apparent, first order reaction. Nonisothermal TGA data are transformed by defining the extent of conversion, $x(t)$, as a function of initial mass, m_i, final mass, m_f, and mass at any time t, m_t:

$$x(t) = \frac{m_i - m_t}{m_i - m_f} \tag{2}$$

A large portion of the biomass pyrolysis literature calculates the activation energy using the reaction rate constant method (RRCM) (see, for example [12,23–25]). In this case, the rate of material reacted at any given time is expressed as a function of the rate constant:

$$\frac{dx(t)}{dt} = k(1 - x(t)) \tag{3}$$

A plot of ln k versus $1/T$, often referred to as an Arrhenius plot, will yield a straight line with a slope of E/R, if the reaction proceeds via an overall first order. Many biomasses, when subjected to analysis via the RRCM, show multiple devolatilization regimes – abrupt changes in slope of the Arrhenius plot at temperatures specific to a given biomass – with each region having its own activation energy. Dozens of biomass pyrolysis studies in the literature show a reaction order of approximately 1; this assumption is commonly applied to account for the simultaneous reactions [26,27].

However, the RRCM fails to capture the entire range of decomposition; for biomass pyrolysis we often see multiple mass loss

regimes over different temperature ranges accounting for the stage-wise decomposition of the primary biomass constituents. That is, the Arrhenius plots have discrete changes in slope that occur over different (but similar) temperature ranges for each biomass. For example, using the RRCM our laboratory found three primary decomposition regions for the pyrolysis of cabbage palm (*Sabal palmetto*), likely corresponding to devolatilization of primarily hemicellulose, cellulose and lignin [28]. However, we know that lignin can devolatilize over a broad temperature range [29], which the limited "mass loss regime" approach of the RRCM cannot elucidate. In addition, there can be substantial (between 2 and 20%) mass lost between one "regime" and another depending on the temperature ramp rate and the temperature range selected for analysis, which is not captured in the RRCM analysis. Selecting a temperature range that encapsulates the most mass loss will decrease the linearity of the mass loss regime segment due to curvature of the line at tail ends, hence the inability to completely capture the entire conversion. Another drawback of the RRCM is the dependence of the activation energy on the temperature ramp rate. At lower temperature mass loss regimes, we find higher activation energies at slower temperature ramp rates; the opposite occurs at high temperature mass loss regimes [28]. Though the differences are often less than 10%, this underscores the importance of noting that activation energies calculated in this manner are likely subject to heat and/or mass transfer limitations, and are thus overall or apparent activation energies at a given heating rate and particle size. For these, and other reasons discussed by the ICTAC Kinetics Committee, isoconversional methods that use at least three temperatures or heating rates, such as the distributed activation energy model, are recommended [30].

A commonality among the many methods used to determine activation energies is the assumption that the countless reactions occurring during pyrolysis are all irreversible first order parallel reactions with different activation energies that occur simultaneously, which can be represented by a distribution function, $f(E)$. The literature is replete with examples of the distributed activation energy model (DAEM) as applied to pure solid fuel pyrolysis, including that of various biomass, coal and other carbonaceous fuels (see, for example [31–36]). The distribution function routinely assumes the form [37,38]:

$$X(t) = 1 - \int_0^\infty \exp\left(-A\int_0^t \exp\left(-\frac{E}{RT}\right)dt\right) f(E)dE \quad (4)$$

If the experiment is conducted nonisothermally at a constant temperature ramp rate, $\beta = dT/dt$, Eq. (4) can be rewritten as:

$$X(t) = 1 - \int_0^\infty \exp\left(-\frac{A}{\beta}\int_0^t \exp\left(-\frac{E}{RT}\right)dT\right) f(E)dE \quad (5)$$

It is commonly assumed that the activation energy is normally distributed with average activation energy, E_a and a standard deviation, σ, whereby:

$$f(E) = \frac{1}{\sigma\sqrt{2\pi}}\exp\left[-\frac{(E-E_a)^2}{2\sigma^2}\right] \quad (6)$$

Non-Gaussian distributions are sometimes used to represent $f(E)$, including Weibull [39], Gamma [40], and Maxwell–Boltzmann [41] distributions.

The frequency factor is often considered to be a constant for all reactions; Miura and Maki [42] allow for a compensation effect between A and E through their Integral method, though Cai et al. [38] question the accuracies of the estimations of A and $f(E)$. However, it stands to reason that a constant frequency factor is also erroneous, as A depends on the collision frequency of molecules during a chemical reaction – that is, it is contingent on the number of molecules present in a control volume – and the success of the collisions between those molecules to result in a reaction. As the amount of molecules participating in pyrolytic reactions increase with temperature and yet decrease as volatiles are lost from the solid, it would seem improbable to expect a constant frequency factor across the range of conversion. In this analysis we determine if synergism exists between these two biomass building blocks, by comparing activation energies obtained using the DAEM across both models and mixture sample sets.

2.3. Evolved compound evolution

To improve the reliability of the evolved compound measurements, we needed to increase the sample size beyond the maximum of ~15 mg possible in the TGA to increase the signal to noise ratio of the quadrupole mass spectrometer (MS). As such, the biomass was pyrolyzed in a 1-in. diameter quartz tube furnace (Lindberg/Blue M®-Mini-Mite) under high purity nitrogen at a flow rate of approximately 105 ± 5 mL/min, monitored by a digital Omega flowmeter. Approximately 0.45 g of sample was placed in a porcelain boat at the center of the hot zone of the furnace, reaching the same relative height in the porcelain boat as in the TGA's crucible. A temperature ramp rate of 10 K/min was used to avoid any diffusion effects arising from heat transfer and to mirror the TGA experiments. Samples were initially heated at 393 K for 30 min to insure moisture removal, and then at 10 K/min up to the final TGA temperature of 1173 K. The exhaust was sampled via a fused silica capillary tubing (40 μm inside diameter) connected to a Quadrupole Mass Spectrometer (Extorr XT Series RGA, XT300M) via a turbomolecular pump at 10^{-7} Torr. The mass spectrometer was in the electron impact (EI) ionization mode at the electron energy of 70 eV and provided mass spectra up to 300 amu. Mass spectrometers are commonly connected to a TGA to measure evolved gases from pyrolysis [43]. It is recognized that the gas volume from biomass pyrolysis is quite limited in the TGA, such that packed bed experiments may present a better picture of total compound evolution [44]. With the tube furnace we were able to use larger samples than in the TGA, and were able to see compounds evolving at lower relative amounts than the small TGA sample sizes allow.

3. Results and discussion

To probe the pyrolysis behavior of cellulose, starch, and their blends, two primary biomass components with the same chemical formula but different structures, we employed thermogravimetric analysis in combination with evolved gas analysis. If these two compounds decompose in an additive manner, we would expect to see a linear relationship between the composition (mass and molar, given that they have equal molecular weights) and activation energy; peak thermal decomposition mass loss rates and temperatures and evolved gas compounds. Conversely, if the compounds react synergistically, promoting or inhibiting thermal decomposition, we would see non-additive trends in the pyrolysis kinetics. If there are chemical reaction synergies between the two compounds, we might encounter variations in non-condensable gases in terms of peak evolution temperatures and concentrations.

3.1. Peak devolatilization temperatures and rates (DTG curves)

Throughout the literature we note a common trend among the devolatilizaiton behavior of many solid fuel blends such as coal and biomass: namely, the peak mass loss rates, as determined through derivative thermogravimetric (DTG) curves, are often an additive combination of the amount of each fuel present [11,45], whereby

Table 2
Derivative thermogravimetric analysis (Peak DTG temperature and mass conversion rate) of cellulose, starch and blends at 10, 50 and 100 K/min.

	10 K/min				50 K/min		100 K/min	
	DTG Peak 1		DTG Peak 2		DTG peak		DTG peak	
	Temp K	Rate s^{-1}	Temp K	Rate s^{-1}	Temp K	Rate s^{-1}	Temp K	Rate s^{-1}
Cellulose	613	5.35E−03			655	4.11E−02	672	1.04E−01
Starch	574	7.06E−03			595	9.83E−02	600	1.89E−01
Mixture 1	612	4.52E−03			655	3.83E−02	660	7.74E−02
Mixture 2	586	3.00E−03	611	3.84E−03	609	3.53E−02	634	7.90E−02
Mixture 3	577	5.19E−03	601	1.58E−03	602	9.11E−02	597	1.33E−01

the peak mass loss rate is linearly proportional to the amount of each component. However, it was unclear if such a trend were to hold for two pure compounds such as starch and cellulose. Table 2 presents the analysis of the DTG curves for the coal–biomass blends investigated each at 10, 50 and 100 K/min. Fig. 1 presents the DTG curves of cellulose, starch and their blends pyrolyzed at these three heating rates.

For pyrolysis at 10 K/min, cellulose decomposes between 290 and 387 °C (563–660 K) with a peak mass conversion rate of $5.35 \times 10^{-3}\ s^{-1}$ at 340 °C (613 K), agreeing with cellulose decomposition values in the literature [17,46]. As expected – given the absence of strong hydrogen bonding – the starch decomposes over a lower temperature range, from 269 °C to 345 °C (542–618 K), and there is one DTG peaks at 574 K corresponding to a conversion rate of $7.06 \times 10^{-4}\ s^{-1}$. These are also in good accord with the literature [5]. At 10 K/min the peak conversion rate is within the same order of magnitude for the cellulose and blends, and is an order of magnitude lower for starch. Though not a linearly additive relationship,

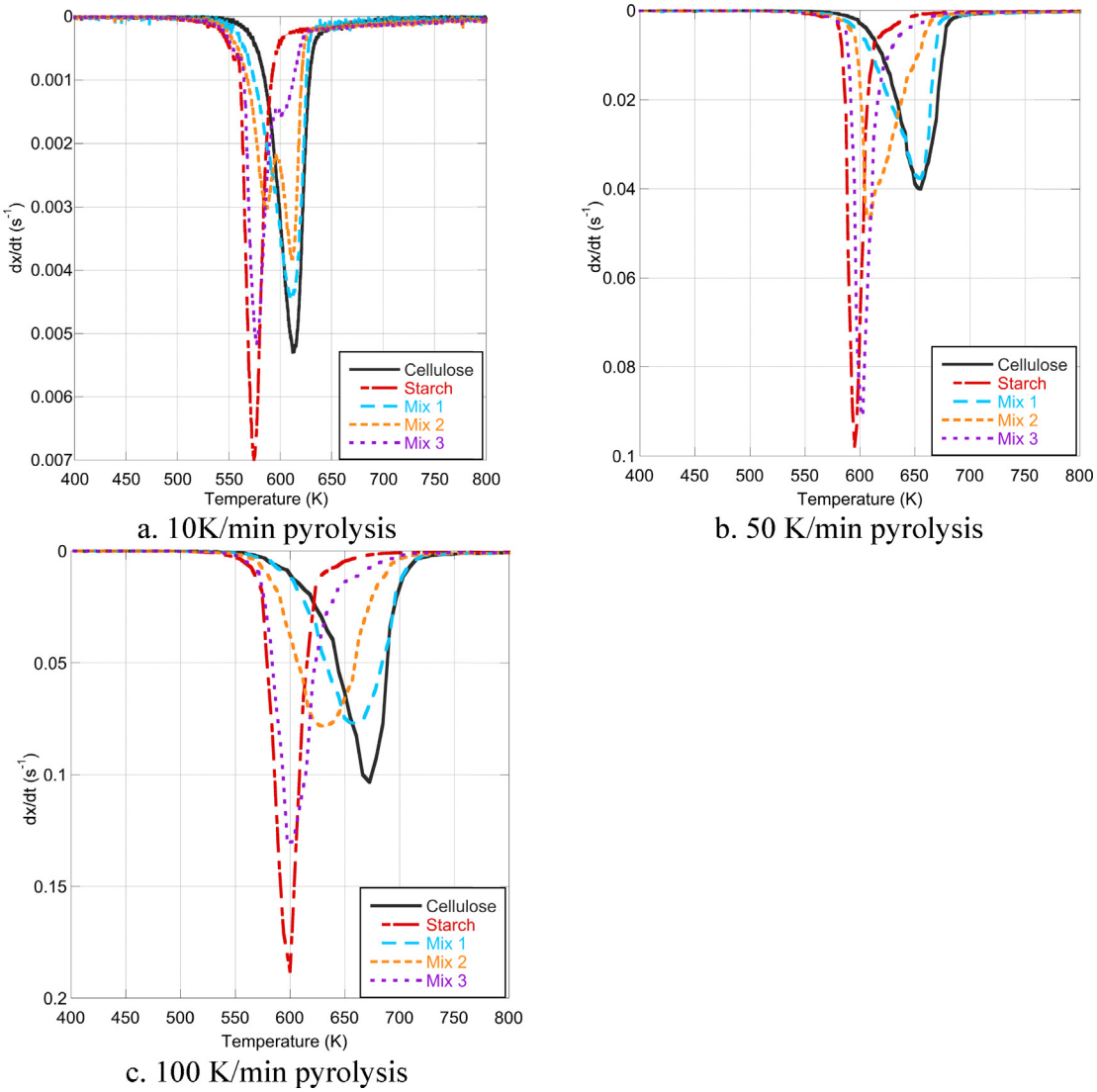

Fig. 1. Derivative thermogravimetric (DTG) curves for cellulose (——), starch (– – –), and blends Mixture 1: 75 wt% cellulose (– –); Mixture 2: 50 wt% cellulose (– – –); Mixture 3: 25 wt% cellulose (– – –), pyrolyzed at 10, 50 and 100 K/min.

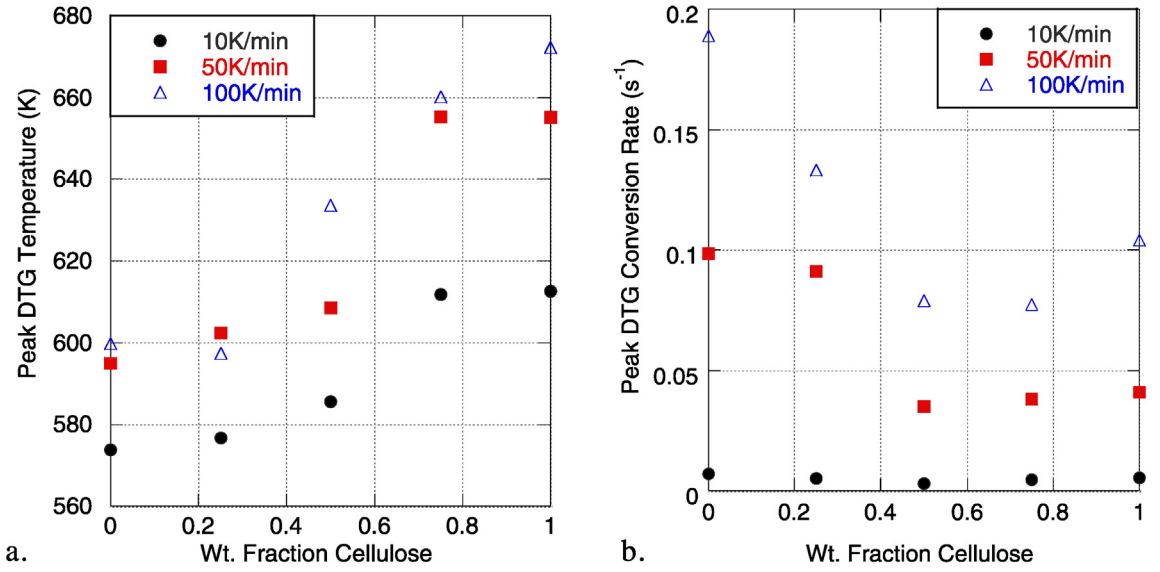

Fig. 2. Peak DTG temperature (a) and conversion rate (b) for pyrolysis of cellulose, starch and blends as a function of mass fraction cellulose at 10 K/min (●); 50 K/min (■); 100 K/min (Δ) (for peak 1 only).

the peak pyrolysis temperature does increase as the percent of cellulose in the mixture increases, as seen in Fig. 2. For example, in the 50:50 mixture, there are two DTG peaks observed. The first is at 586 K – almost 12 K higher than pure starch, but 27 K lower than pure cellulose; the second peak is at 611 K – the same temperature as the cellulose peak. This suggests that the cellulose is slowing the devolatlizaiton of the starch in the mixture at this composition while it itself is not impacted. Conversely, in Mixture 3 (75 wt% starch), the first peak occurs a mere 3 K higher than the pure starch, and second peak at 601 K – suggesting that the starch devolatlization is not impacted by the presence of cellulose, yet the cellulose decomposes at a lower temperature, though same order of magnitude in rate, as compared to pure cellulose. Finally, when cellulose is the dominant mixture component, we see only one DTG peak at roughly the same temperature and rate as the pure cellulose, suggesting that the decomposition kinetics of the cellulose control the blends' overall decomposition.

When we increase the heating rate to 50 K/min, cellulose decomposes from 308 °C to 439 °C (581–712 K), and there is a single DTG peak observed at 382 °C (655 K) with a rate of $4.11 \times 10^{-2}\ s^{-1}$. For the starch, the pyrolysis process mainly occurs in the temperature range from 304 °C to 367 °C (577–640 K), and there is only one peak at 322 °C (595 K) with a rate of $9.83 \times 10^{-2}\ s^{-1}$. For pyrolysis at 100 K/min, cellulose decomposes from 293 °C to 448 °C (566–721 K), and there is one peak at 399 °C (672 K) (Table 2). The corresponding peak conversion rate is $0.104\ s^{-1}$. For the starch, the pyrolytic decomposition spans the temperature range of 286 °C to 387 C (559–660 K), with one peak at 327 °C (600 K) at a conversion rate of $0.189\ s^{-1}$. As with the 10 K/min pyrolysis, the peak temperature for 50 and 100 K/min pyrolysis increases following an increase of the percentage of cellulose in the mixture while the opposite trend occurs for peak DTG conversion rate. However, as can be seen in Fig. 2, the peak rate of decomposition is highest for the pure starch at 50 and 100 K/min, in opposition to the 10 K/min results.

With the exception of Mixture 3, the peak temperatures increase following the increase of heating rate for all of the samples (the peak DTG temperature of Mixture 3, 25 wt% cellulose, is slightly lower for the 100 K/min than the 50 K/min heating rate – a difference of 7 °C). Overall this is not an unexpected relationship – the slower the heating rate, the more time each sample has to react at each temperature. In a similar vein, the peak reaction rate is highest at 100 K/min and lowest at 10 K/min pyrolysis. Interestingly, the

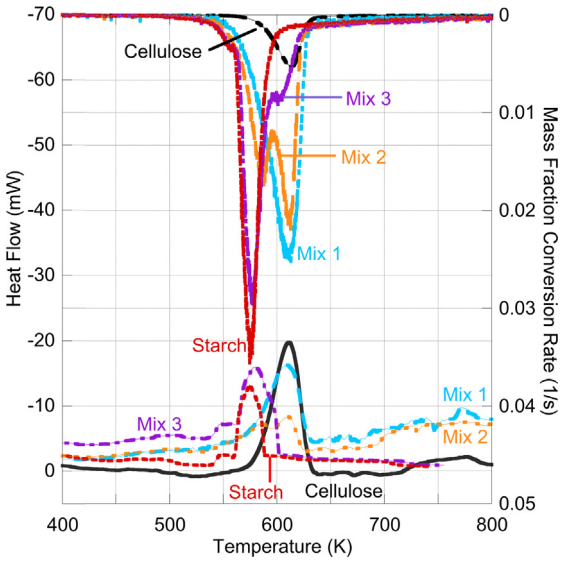

Fig. 3. Combined DTG/DSC plot for cellulose, starch and mixtures.

relationships between both peak temperature and peak conversion rate and the blend weight fraction of cellulose are not "additive" in nature. The peak reaction rate of pure starch is considerably higher at 50 and 100 K/min than that of pure cellulose. It appears that as the fraction of cellulose increases beyond 50 wt% in the mixture, the peak reaction rate is decreased by the presence of the cellulose in the mixture beyond a simple additive trend. This behavior is magnified when we look at the combined DTG–DSC curves, as seen in Fig. 3 for the 10 K/min pyrolysis. In this case we see that the DTG peaks correspond to the endothermic troughs for each solid and blend. Pure starch has a gradually decreasing endotherm from ~600 to 950 K, with a sharp decline after 950 K. The 75 wt% starch mixture (Mixture 3) follows this heat flow curve. The pure cellulose curve, on the other hand, remains fairly flat between 625 and 800 K, then has a slight exothermic peaks and then falls gradually at 900 K. Similar behavior was noted by Yang et al. for the pyrolysis of pure cellulose [44]. Likewise, the 75 wt% and 50 wt% cellulose mixtures more closely follow the shape of the cellulose endotherm, though both dip below the cellulose to a small trough at ~875 K and peak

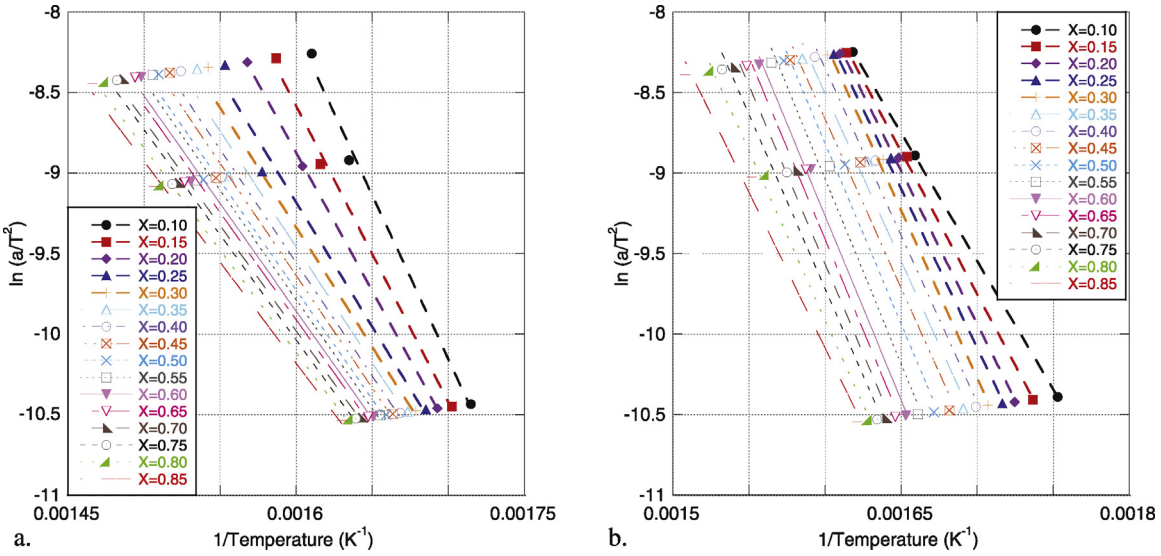

Fig. 4. Representative isoconversional plots for pure cellulose and 50:50 mixture at mass fractional conversions X = (●) 0.1; (▪) 0.15; (◆) 0.20; (▲) 0.25; (+) 0.30; (△) 0.35; (○) 0.40; (☒) 0.45; (▯) 0.50; (□) 0.55; (▼) 0.60; (▽) 0.65; (◣) 0.70; (⊙) 0.75; (◢) 0.80; (▬) 0.85.

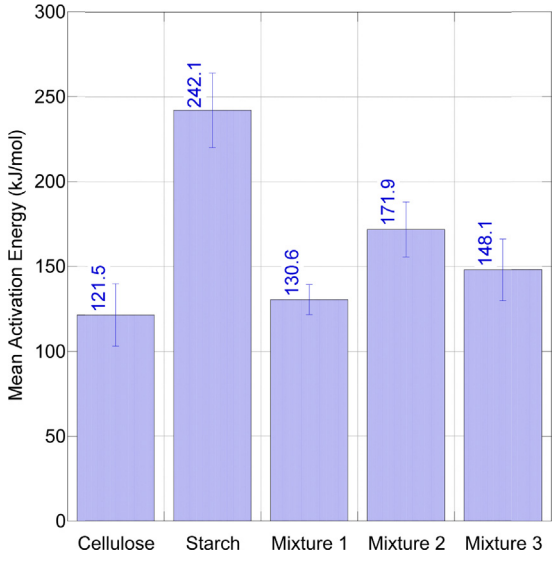

Fig. 5. Mean activation energy for each pure sample and blend calculated via DAEM (error bars represent 1 standard deviation).

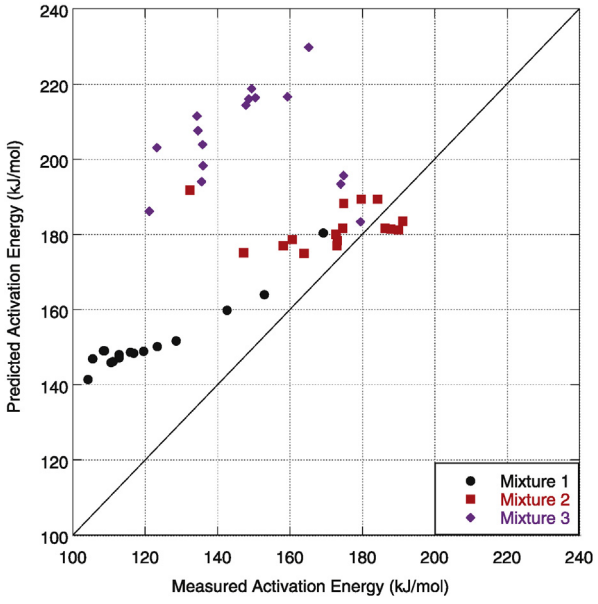

Fig. 6. Predicted (Eq. (4)) versus measured (DAEM) activation energy at each mass fraction conversion level for starch–cellulose mixtures.

around 1000 K before tapering off to meet the pure cellulose curve. The DSC data therefore also point to a non-additive thermal degradation (DSC data for 50 and 100 K/min pyrolysis available in online Supplemental Information). To further explore this potential reaction synergy between these two glucose biomass building blocks, we turn our attention to global activation energies as calculated via an isoconversional method.

3.2. Activation energy of starch–cellulose blends

As heating rate has a significant impact on activation energies of even these pure biomass components, we turn to an isoconversional analysis of the data using the distributed activation energy model to remove this experimental variable from our analysis of reaction synergism. Overall good linearity was found for each pure compound and blend using the integral method of the DAEM, illustrated in Fig. 4.

Activation energies of each pure compound and blend were determined at mass fractional conversions from 0.10 to 0.85 at intervals of 0.05, detailed in Table 3 (full analysis with slope, intercept, and regression coefficients provided in the Supplemental Information, Table S1; results presented graphically in Supplemental Fig. S2).

For the pyrolysis of pure cellulose, we find activation energies ranging from 104.2 ± 6.9 to 169.2 ± 12.8 kJ/mol. For pure starch the DAEM returned activation energies between 197.2 ± 69.7 and 270.9 ± 34.3 kJ/mol. This range of values – and indeed the average activation energies (Fig. 5) measured – is in agreement with the vast pure cellulose pyrolysis literature. Using a first order Arrhenius model, literature values of the activation energy of pure cellulose range from 110.0 kJ/mol [47] to 238.0 kJ/mol [48]. Hashimoto et al. [49] report activation energy of 167.7 kJ/mol via a nonlinear

Table 3
Activation energies and pre-exponential factors for each pure fuel and blend determined via the Distributed Activation Energy Model.

Conversion	E_a (kJ/mol)	A (s^{-1})	E_a (kJ/mol)	A (s^{-1})
Cellulose			Mixture 2	
0.10	169.2 ± 12.8	4.10E+10 ± 1.26E+01	132.3 ± 0.6	4.00E+07 ± 2.16E+00
0.15	153.0 ± 8.7	1.14E+09 ± 5.56E+00	147.2 ± 4.4	6.86E+08 ± 2.42E+00
0.20	142.7 ± 1.7	1.19E+08 ± 1.39E+00	158.1 ± 7.0	5.30E+09 ± 4.04E+00
0.25	128.5 ± 17.1	5.60E+06 ± 2.72E+01	163.9 ± 7.6	1.51E+10 ± 4.52E+00
0.30	123.4 ± 17.4	1.82E+06 ± 2.84E+01	173.0 ± 9.5	7.99E+10 ± 6.59E+00
0.35	119.6 ± 20.8	7.78E+05 ± 5.29E+01	173.2 ± 21.7	6.00E+10 ± 7.12E+01
0.40	116.9 ± 15.1	4.19E+05 ± 1.77E+01	172.8 ± 15.4	6.61E+10 ± 2.08E+01
0.45	115.9 ± 12.6	3.19E+05 ± 1.10E+01	174.6 ± 29.3	6.77E+10 ± 3.09E+02
0.50	112.8 ± 13.7	1.61E+05 ± 1.33E+01	186.3 ± 23.8	5.55E+11 ± 1.03E+02
0.55	112.8 ± 14.0	1.50E+05 ± 1.39E+01	191.1 ± 22.1	1.11E+12 ± 7.18E+01
0.60	111.1 ± 11.3	1.01E+05 ± 8.34E+00	189.9 ± 11.6	7.11E+11 ± 9.25E+00
0.65	110.5 ± 11.5	8.61E+04 ± 8.55E+00	187.9 ± 21.7	4.17E+11 ± 6.48E+01
0.70	108.7 ± 8.8	5.62E+04 ± 5.14E+00	184.2 ± 24.8	1.74E+11 ± 1.14E+02
0.75	108.5 ± 8.8	5.17E+04 ± 5.18E+00	179.7 ± 25.0	6.29E+10 ± 1.15E+02
0.80	105.5 ± 9.4	2.69E+04 ± 5.66E+00	174.9 ± 10.3	2.04E+10 ± 7.01E+00
0.85	104.2 ± 6.9	1.94E+04 ± 3.56E+00	160.6 ± 16.5	1.11E+09 ± 2.20E+01
Starch			Mixture 3	
0.10	214.2 ± 22.9	1.89E+15 ± 1.14E+02	123.2 ± 9.1	1.01E+07 ± 6.52E+00
0.15	197.2 ± 69.7	3.54E+13 ± 1.57E+06	121.1 ± 15.4	5.20E+06 ± 2.30E+01
0.20	211.1 ± 66.2	5.07E+14 ± 7.15E+05	135.6 ± 18.2	8.06E+07 ± 3.93E+01
0.25	221.5 ± 68.8	3.60E+15 ± 1.18E+06	136.0 ± 24.4	8.29E+07 ± 1.36E+02
0.30	230.6 ± 59.2	1.99E+16 ± 1.62E+05	135.9 ± 23.8	7.40E+07 ± 1.19E+02
0.35	236.9 ± 56.4	6.25E+16 ± 8.80E+04	134.6 ± 22.4	5.24E+07 ± 8.85E+01
0.40	243.1 ± 53.0	1.91E+17 ± 4.33E+04	134.3 ± 21.7	4.55E+07 ± 7.67E+01
0.45	247.2 ± 49.1	3.89E+17 ± 1.92E+04	147.8 ± 32.9	7.26E+08 ± 7.23E+02
0.50	250.3 ± 39.5	6.28E+17 ± 2.75E+03	148.6 ± 33.0	7.79E+08 ± 7.36E+02
0.55	254.1 ± 38.6	1.16E+18 ± 2.26E+03	149.4 ± 33.2	8.43E+08 ± 7.50E+02
0.60	251.4 ± 31.0	5.51E+17 ± 4.79E+02	150.5 ± 33.5	9.38E+08 ± 7.70E+02
0.65	252.0 ± 25.4	4.78E+17 ± 1.53E+02	159.3 ± 41.7	5.20E+09 ± 3.86E+03
0.70	270.2 ± 31.4	1.15E+19 ± 4.81E+02	165.2 ± 46.9	1.45E+10 ± 1.05E+04
0.75	270.2 ± 35.8	5.73E+19 ± 1.41E+03	174.8 ± 56.9	8.08E+10 ± 7.27E+04
0.80	270.9 ± 34.3	5.47E+19 ± 1.02E+03	174.1 ± 52.9	5.10E+10 ± 3.09E+04
0.85	252.9 ± 24.5	1.12E+18 ± 1.38E+02	179.5 ± 57.6	1.15E+11 ± 6.91E+04
Mixture 1				
0.10	143.5 ± 18.6	2.65E+08 ± 4.07E+01		
0.15	138.7 ± 18.0	7.39E+07 ± 3.51E+01		
0.20	138.0 ± 11.2	5.11E+07 ± 8.90E+00		
0.25	135.7 ± 8.5	2.73E+07 ± 5.20E+00		
0.30	135.7 ± 15.5	2.27E+07 ± 1.98E+01		
0.35	139.3 ± 13.7	4.13E+07 ± 1.41E+01		
0.40	138.0 ± 15.4	2.78E+07 ± 1.92E+01		
0.45	133.4 ± 13.1	9.95E+06 ± 1.22E+01		
0.50	132.4 ± 9.9	7.51E+06 ± 6.60E+00		
0.55	131.4 ± 6.8	5.59E+06 ± 3.64E+00		
0.60	126.0 ± 5.2	1.77E+06 ± 2.67E+00		
0.65	123.8 ± 2.6	1.07E+06 ± 1.63E+00		
0.70	123.0 ± 0.4	8.36E+05 ± 1.07E+00		
0.75	121.0 ± 2.9	5.34E+05 ± 1.72E+00		
0.80	115.9 ± 3.9	1.81E+05 ± 2.08E+00		
0.85	113.8 ± 6.2	1.14E+05 ± 3.16E+00		

least squares analysis of nonisothermal data; "semi-global" models yield values ranging from 61.0 kJ/mol [50] to 242.4 kJ/mol [51]. Finally, isoconversional models show a variety of activation energies, from 164.0 kJ/mol [52] to 175.6 kJ/mol via the DAEM [53].

Using the DAEM calculated activation energies, we predicted, via Eq. (4), an activation energy as a function of blend composition at each mass fraction conversion, plotted against the measured activation energy in Fig. 6. We find that deviations from predicted values are all above the $y = x$ line, such that the predicted values are, with the exception of a few points for Mixture 2, all higher than the measured values. This suggests some sort of synergy between the two components. However, it is not clear whether the two compounds are interacting chemically or physically; is the "interaction" behavior due to chemical interactions of volatiles promoting reaction among the solids, or is it a transport limitation related to the higher activation energy barrier for cellulose to pyrolyze versus starch? We turn to an analysis of the primary gas components evolved during pyrolysis to probe this behavior further.

3.3. Gaseous products evolved from pyrolysis

The evolved gases: H_2, CH_4, C_2H_2, C_2H_6 and CO_2 (corresponding to AMU signals of 2, 16, 26, 30 and 44, respectively) were monitored in this study by pyrolyzing 400 ± 30 mg each of the pure compounds and mixtures in a tube furnace at 10 K/min (the maximum heating rate of the furnace) with high purity nitrogen flowing at 105 ± 5 mL/min through the furnace. The data are presented in Table 4 using natural logarithm form of the ratio of the evolved gas divided by the sum of the gases (log of the partial pressure = log concentration), normalized to the fraction of total sample converted (between 0.818 for Mixture 2 and 0.864 for pure starch.)

Fig. 7 presents relative concentrations of each evolved gas marker compound as a function of temperature.

Table 4
Peak temperatures and concentrations normalized to fraction devolatilized of gaseous species evolved for each pure compound and mixture.

	H_2 Peak 1		H_2 Peak 2	
	Temp (K)	Log Pi/*P*	Temp (K)	Log Pi/*P*
Cellulose	642.7	9.57E−09	1055.5	1.46E−07
Starch	586.0	1.33E−08	1035.7	2.53E−07
Mixture 1	619.3	1.49E−08	1033.8	2.42E−07
Mixture 2	605.6	1.78E−08	1041.6	2.78E−07
Mixture 3	597.8	1.12E−08	1039.7	2.32E−07
	C_2H_2 Peak 1		C_2H_2 Peak 2	
	Temp (K)	Log Pi/*P*	Temp (K)	Log Pi/*P*
Cellulose	640.8	1.13E−09	758.1	1.14E−09
Starch	584.1	1.44E−09	734.6	2.15E−09
Mixture 1	617.3	1.70E−09	738.4	2.12E−09
Mixture 2	607.5	1.91E−09	738.5	2.32E−09
Mixture 3	619.3	9.71E−10	746.4	1.89E−09
	CH_4 Peak 1		CH_4 Peak 2	
	Temp (K)	Log Pi/*P*	Temp (K)	Log Pi/*P*
Cellulose	634.9	1.32E−08	830.4	1.11E−08
Starch	582.1	3.40E−08	805.0	2.18E−08
Mixture 1	613.4	2.61E−08	805.3	2.03E−08
Mixture 2	603.6	3.07E−08	803.1	1.93E−08
Mixture 3	603.6	1.88E−08	807.0	1.86E−08
	C_2H_6 Peak 1		C_2H_6 Peak 2	
	Temp (K)	Log Pi/*P*	Temp (K)	Log Pi/*P*
Cellulose	609.5	9.43E−10	756.1	1.04E−09
Starch	580.2	9.57E−10	734.6	1.26E−09
Mixture 1	611.5	1.07E−09	738.5	1.32E−09
Mixture 2	603.6	1.19E−09	740.5	1.53E−09
Mixture 3	599.7	9.02E−10	746.4	1.23E−09
	CO_2 peak			
	Temp (K)	Log Pi/*P*		
Cellulose	634.9	9.57E−08		
Starch	582.1	2.83E−07		
Mixture 1	613.4	2.03E−07		
Mixture 2	601.7	2.37E−07		
Mixture 3	599.9	1.43E−07		

Fig. S1 (Supplemental Information) shows the concentration of each evolved gas as a function of temperature with overlaid heat flow data for each compound and mixture. For cellulose, there is a primary peak of evolved CO_2 at 638 K, approximately 25 K higher than the primary DTG peak at 612.5 K. As cellulose decomposes, there are two peaks for H_2 evolution. The first is at 642.7 K and second at 1055.5 K. Likewise, there are two peaks for CH_4, C_2H_2 and C_2H_6 evolution. Cellulose has the highest peak evolution temperatures for all of the gases monitored, and starch has the lowest peak temperatures for each gas.

Of note is the correlation between the first peak temperature for each evolved gas species and the fraction of cellulose present in the blend (Table 5). These two variables have correlation coefficients, R^2, for simple linear regression models ("additive schemes") for H_2, CH_4, and CO_2 greater than 0.90, with a somewhat looser relationship for C_2H_2 and C_2H_6 ($R^2 > 0.70$). However, as seen in Fig. 8, this is clearly not the case for the second peak evolution temperatures, where correlation coefficients are all less than 0.45.

There is a loose correlation between peak DTG temperature and peak evolution temperature for any gaseous species, and in the expected direction. As temperature is increasing at a rate of 10 K/min, we would expect the peak mass loss of the sample to occur several degrees (and therefore seconds) before the evolved gases are detected in the MS because (1) there will be a lag as evolving compounds travel the capillary compound and reach the detector and (2) as gases devolatilize from the solid, they must diffuse out of the pores and from the surface of the solid sample, which gives them ample time to experience secondary cracking. Fig. S1 in the online supplemental information shows that such a trend continues through the peak endothermic behavior. That is, the peak endotherms (requiring the highest amount of heat to complete the reaction at this point) loosely correspond to the first peaks in each of the evolved gas components.

We note no apparent relationship between the peak concentrations and cellulosic fraction, with the general exception that the pure cellulose has the lowest concentrations of any sample, though within the same order of magnitude for each solid. This is illustrated graphically in Fig. 9. Yang et al. [44], using FTIR to monitor evolved gases, found that the total gaseous pyrolysis products released from cellulose were lower than those devolatilizing from hemicellulose. Hosoya et al. [54] found slightly lower tar yield and slightly higher char yield by mixing in a 2:1 cellulose:hemicellulose mixture than would be predicted in an additive scheme, which the authors suggest is because cellulose is covered by a molten hemicellulose phase, inhibiting volatile formation from the cellulose. Given the high volume expansion of starch, and the observation that the total mass conversion of all the samples was approximately equal, we do not believe the lower (though same order of magnitude) concentrations of H_2, CH_4, C_2H_2, C_2H_6 and CO_2, of cellulose and mixtures higher in cellulose is due to an analogous

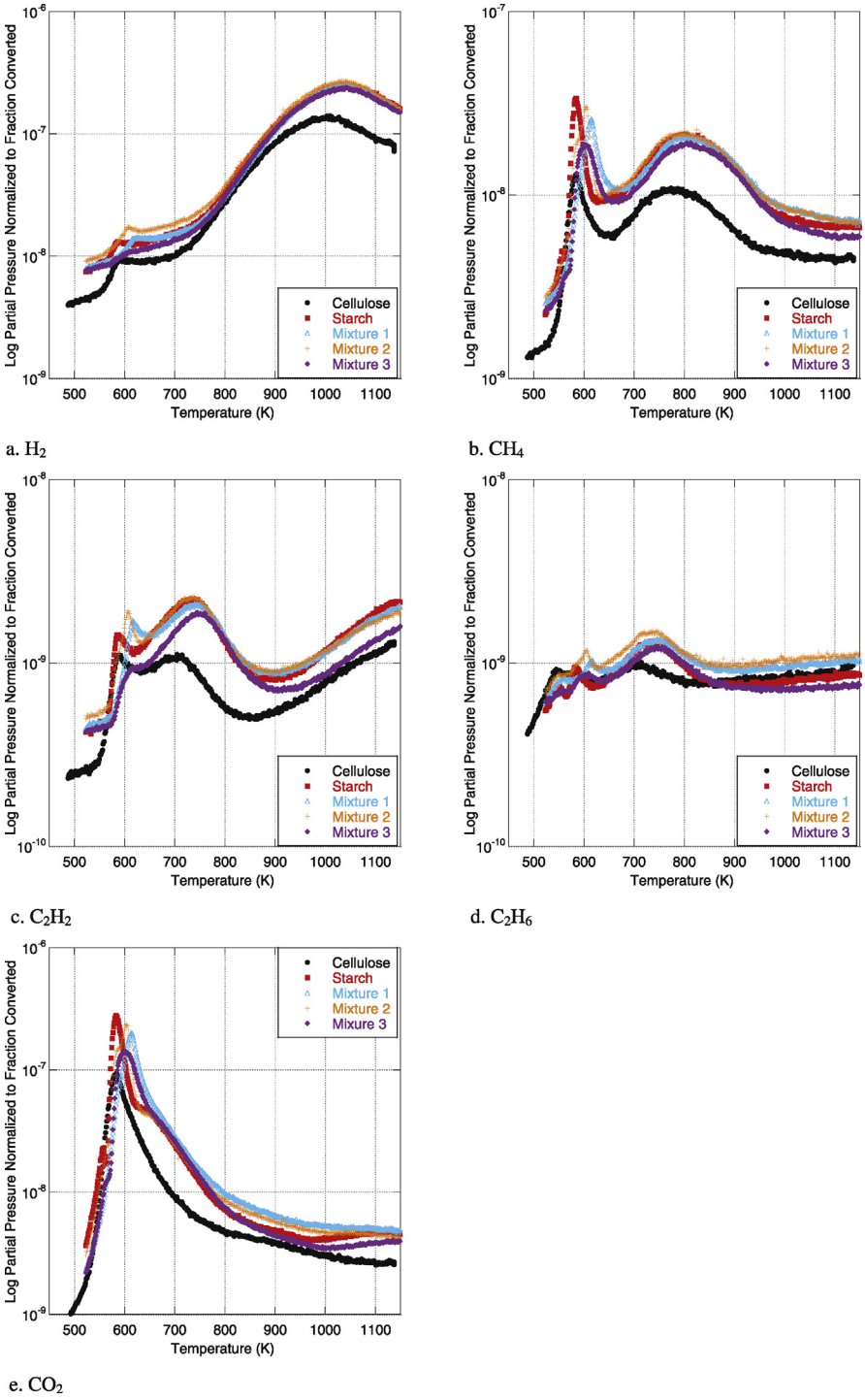

Fig. 7. Log of evolved gas concentrations from pyrolysis of cellulose, starch, and blends at 10 K/min for cellulose (●), starch (■), and blends Mixture 1: 75 wt% cellulose (△); Mixture 2: 50 wt% cellulose (+); Mixture 3: 25 wt% cellulose (◆). (a) H_2, (b) CH_4, (c) C_2H_2, (d) C_2H_6 and (e) CO_2.

Table 5
Linear regression equations for relationship between peak evolved gas temperature and mass fraction of cellulose.

	Linear regression equation	R	R^2
H_2 Peak 1	Peak T (K) = $53.96 \pm 6.52 \times (x_{cellulose}) + 583.30 \pm 3.99$	0.97877	0.95799
H_2 Peak 2	Peak T (K) = $13.48 \pm 9.75 \times (x_{cellulose}) + 1034.50 \pm 5.97$	0.62377	0.38909
CH_4 Peak 1	Peak T (K) = $46.16 \pm 8.31 \times (x_{cellulose}) + 584.44 \pm 5.09$	0.95468	0.91141
CH_4 Peak 2	Peak T (K) = $19.64 \pm 12.19 \times (x_{cellulose}) + 800.34 \pm 7.47$	0.68107	0.46386
C_2H_2 Peak 1	Peak T (K) = $44.56 \pm 15.53 \times (x_{cellulose}) + 591.52 \pm 9.51$	0.85609	0.73289
C_2H_2 Peak 2	Peak T (K) = $15.6 \pm 10.31 \times (x_{cellulose}) + 735.4 \pm 6.31$	0.65796	0.43291
C_2H_6 Peak 1	Peak T (K) = $28.16 \pm 8.26 \times (x_{cellulose}) + 586.82 \pm 5.06$	0.89154	0.79484
C_2H_6 Peak 2	Peak T (K) = $14.04 \pm 9.14 \times (x_{cellulose}) + 736.2 \pm 5.60$	0.66334	0.44002
CO_2 Peak	Peak T (K) = $47.64 \pm 7.21 \times (x_{cellulose}) + 582.58 \pm 4.42$	0.96728	0.93563

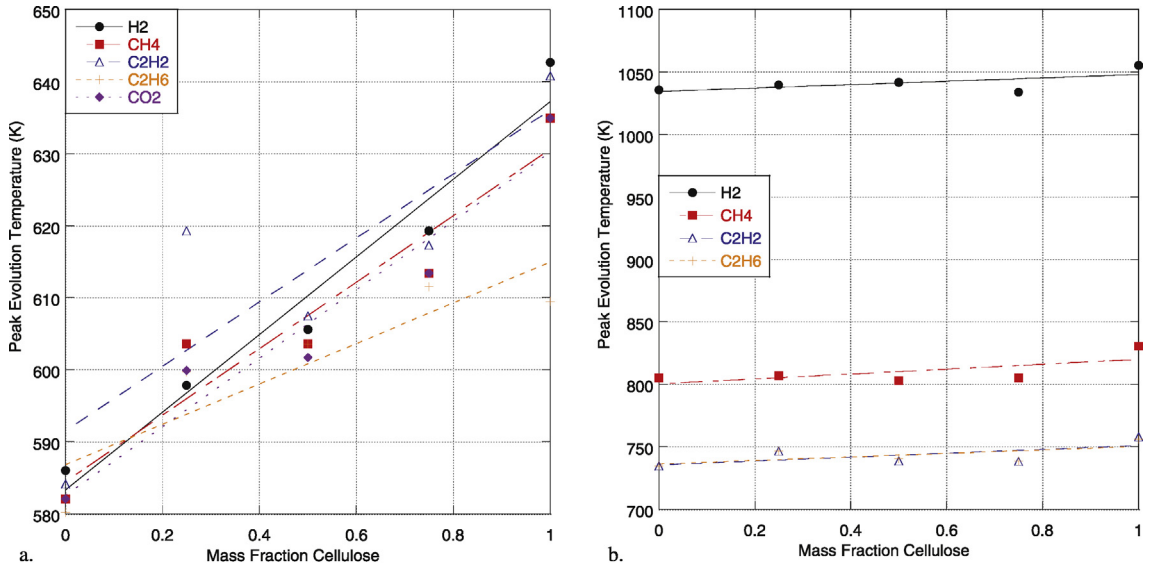

Fig. 8. Temperatures of peak evolution of evolved gases as a function of mass fraction of cellulose for each pure compound and mixture pyrolyzed at 10 K/min: H_2 (●), CH_4 (■), C_2H_2 (Δ), C_2H_6 (+), CO_2 (◆).

liquid-phase shielding effect. In addition, from the fairly linear behavior for the first peak, it would appear that initially the blended streams do not display evidence of reaction synergism between the starch and cellulose during co-pyrolysis in terms of the non-condensable gases formed. Rather, it is likely that the cellulosic gases underwent repolymerization of anhydrosugars, increasing tar yield and decreasing non-condensable gas yield, which is supported through the non-linear relationship for the second peak devolatilization as observed in Table 5.

3.4. Kinetics and evolved gases: two sides to the synergism story

Starch and cellulose represent the building blocks of many biomasses, and provide a foundational understanding of how different biomass constituents may influence pyrolytic decomposition. There is no obvious chemical pathway by which starch and cellulose, two glucose isomers and building blocks of many biomasses, interact during pyrolysis. There is evidence in terms of reaction rates and kinetics that the cellulose, when present as the majority component (75 wt%) inhibits the devolatilization of starch, and perhaps at higher starch fractions the rates of reaction are higher than a simple additive scheme would predict. Activation energies are not additive in nature, suggesting some sort of synergism between the two components.

However, given the lack of chemical reaction synergism noted for the first devolatilization peak – there is no evidence that the evolved (noncondensable) gas profiles are drastically altered as a result of the blends – we suggest that the synergies noted in terms of reaction kinetics are initially due to heat transport and diffusional issues between the particles. For the 25 wt% cellulose and 50 wt% cellulose mixtures, the peak derivative thermogravimetric temperatures and rates indicate that the starch is perhaps promoting devolatilization of the cellulose; the peak temperatures are lower than predicted and peak rates higher than predicted by an additive model. For the 75 wt% cellulose mixture, we see temperature considerable higher and rate considerably lower than

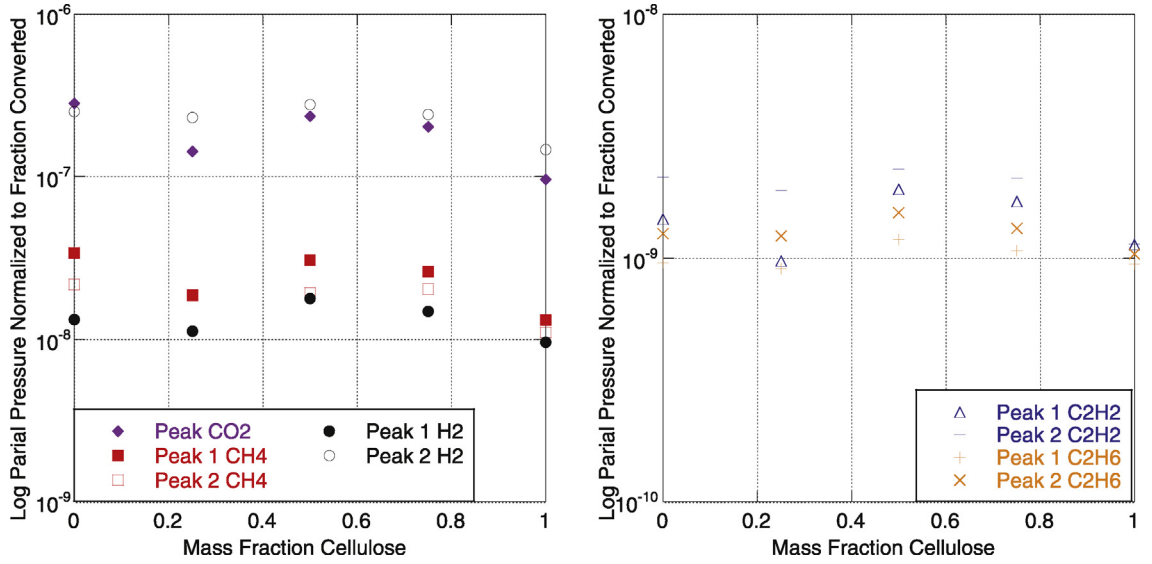

Fig. 9. Peak evolved gas concentration, normalized to total fraction evolved compounds as a function of mass fraction of cellulose for each pure compound and mixture pyrolyzed at 10 K/min: H_2 Peak 1 (●), H_2 Peak 2 (○), CH_4 Peak 1(■), CH_4 Peak 2 (□), Peak CO_2 (◆), C_2H_2 Peak 1 (Δ), C_2H_2 Peak 2 (—), C_2H_6 Peak 1 (+), C_2H_6 Peak 2 (X).

would be predicted by an additive scheme, especially at the 50 and 100 K/min heating rates. This is further underscored by the differential scanning calorimetry results, where we see sharper and deeper endotherms for cellulose and the 75 wt% cellulose mixture than the 50:50, 25 wt% cellulose and pure starch samples. The primary peak evolved gas temperatures and mass fractions of cellulose in a mixture are strongly correlated; as the percentage of cellulose increases, the temperatures at which the peak mass loss and peak evolved gases emerge are linearly related. As such, there is not substantial evidence pointing to a high degree of chemical reaction synergism during the pyrolysis of these two biomass building blocks at lower temperatures. However, at higher temperatures, the relationship between cellulose fraction and peak evolved gases is not linear in nature. The most logical explanation for the behavior is the cellulose undergoing char-forming side reactions [55,56], which may inhibit starch devolatilization and increase peak pyrolysis temperatures. As Várhegyi explains, unfortunately the physical properties (i.e. transport) of a solid sample change with temperature, and of course in our case, mixture composition likely compounds this phenomenon [57]. We presume – like all similar TGA experiments – that the samples are under kinetic control during the experiments, i.e. devolatilization and product formation is governed by chemical reactions and not transport properties. However, the synergism in terms of mass loss data and lack thereof for pyrolysis gas data at lower temperatures, and synergism for both data sets at higher temperatures, suggests that there might be both kinetic and transport forces at play between these two biomass building blocks, especially at lower temperatures. This interplay is understood through the significantly higher heat capacity and peak devolatilization temperatures of cellulose versus starch, whereby a mixture with a significant amount of cellulose may suppress the ability of starch to devolatilize at lower temperatures.

4. Conclusions

There is much evidence in the literature that blending biomass and other solid fuel streams can alter reaction rates and temperatures – as observed here – that can potentially increase conversion efficiency. For example, mixtures of 50% or more of starch appear to promote the pyrolysis of cellulose at lower temperatures. In addition, there is a consensus developing that we can advantageously alter bio-oil composition by blending biomasses to improve stability and fuel quality. However, what the data here suggest is that this reaction synergy may not be due to a chemical interaction occurring during devolatilization, at least not at lower temperatures. Rather, the ability to tune bio-oil product composition is likely due to secondary reactions occurring to form or change tar phase constituents.

Acknowledgement

The authors acknowledge the generous support of the scholarship from China Scholarship Council (CSC) under the Grant CSC NO. 201406350169.

Appendix A. Supplementary data

Supplementary data associated with this article can be found, in the online version, at http://dx.doi.org/10.1016/j.tca.2015.09.002.

References

[1] N. Kauffman, D. Hayes, R. Brown, A life cycle assessment of advanced biofuel production from a hectare of corn, Fuel 90 (2011) 3306–3314.
[2] A. Oasmaa, C. Peacocke, S. Gust, D. Meier, R. McLellan, Norms and standards for pyrolysis liquids. End-user requirements and specifications, Energy Fuels 19 (2005) 2155–2163.
[3] J.F. González, J.M. Encinar, J.L. Canito, E. Sabio, M. Chacón, Pyrolysis of cherry stones: energy uses of the different fractions and kinetic study, J. Anal. Appl. Pyrolysis 67 (2003) 165–190.
[4] F. de Miguel Mercader, M.J. Groeneveld, S.R.A. Kersent, R.H. Venderbosch, J.A. Hogendoorn, Pyrolysis oil upgrading by high pressure thermal treatment, Fuel 89 (2010) 2829–2837.
[5] T. Cornelissen, M. Jans, M. Stals, T. Kuppens, T. Thewys, G.K. Janssens, H. Pastijn, J. Yperman, G. Reggers, S. Schreurs, R. Carleer, Flash co-pyrolysis of biomass: the influence of biopolymers, J. Anal. Appl. Pyrolysis 85 (2009) 87–97.
[6] C. Meesri, B. Moghtaderi, Lack of synergistic effects in the pyrolytic characteristics of woody biomass/coal blends under low and high heating rate regimes, Biomass Bioenergy 23 (2002) 55–66.
[7] A.K. Sadhukhan, P. Gupta, T. Goyal, R.K. Saha, Modelling of pyrolysis of coal–biomass blends using thermogravimetric analysis, Bioresour. Technol. 99 (2008) 8022–8026.
[8] A.O. Aboyade, M. Carrier, E.L. Meyer, J.H. Knoetz, J.F. Görgens, Model fitting kinetic analysis and characterization of the devolatilization of coal blends with corn and sugarcane residues, Thermochim. Acta 530 (2012) 95–106.
[9] Q. Liu, Z. Zhong, S. Wang, Z. Luo, Interactions of biomass components during pyrolysis: a TG-FTIR study, J. Anal. Appl. Pyrolysis 90 (2011) 213–218.
[10] T. Sonobe, N. Worasuwannarak, S. Pipatmanomai, Synergies in co-pyrolysis of Thai lignite and corncob, Fuel Process. Technol. 89 (2008) 1371–1378.
[11] A.M. Celaya, A.T. Lade, J.L. Goldfarb, Co-combustion of brewer's spent grains and Illinois no 6 coal: impact of blend ratio on pyrolysis and oxidation behavior, Fuel Process. Technol. 129 (2015) 39–51.
[12] P. Yangali, A.M. Celaya, J.L. Goldfarb, Co-pyrolysis reaction rates and activation energies of West Virginia coal and cherry pit blends, J. Anal. Appl. Pyrolysis 108 (2014) 203–211.
[13] L. Petrus, M.A. Noordermeer, Biomass to biofuels, a chemical perspective, Green Chem. 8 (2006) 861–867.
[14] P. Aggarwal, D. Dollimore, A comparative study of the degradation of different starches using thermal analysis, Talanta 43 (1996) 1527–1530.
[15] A.A.A. Soliman, N.A. El-Shinnawy, F. Mobarak, Thermal behavior of starch and oxidized starch, Thermochim. Acta 296 (1997) 149–153.
[16] X. Liu, L. Yu, F. Xie, M. Li, L. Chen, X. Li, Kinetics and mechanism of thermal decomposition of cornstarches with different amylose/amylopectin ratios, Starch 62 (2010) 139–146.
[17] D.F. Arseneau, Competitive reactions in the thermal decomposition of cellulose, Can. J. Chem. 49 (1971) 632–638.
[18] H. Yang, R. Yan, H. Chen, C. Zheng, D.H. Lee, D.T. Liang, In-depth investigation of biomass pyrolysis based on three major components: hemicellulose, cellulose, and lignin, Energy Fuels 20 (2006) 388–393.
[19] B.G. Girija, R.R.N. Sailaja, S. Biswas, M.V. Deepthi, Mechanical and thermal properties of Eva blended with biodegradable ethyl cellulose, J. Appl. Polym. Sci. 116 (2010) 1044–1056.
[20] W. Jiang, X. Qiao, K. Sun, Mechanical and thermal properties of thermoplastic acetylated starch/poly(ethylene-*co*-vinyl alcohol) blends, Carbohydr. Polym. 65 (2006) 139–143.
[21] J.F. Mano, D. Koniarova, R.L. Reis, Thermal properties of thermoplastic starch/synthetic polymer blends with potential biomedical applicability, J. Mater. Sci.: Mater. Med. 14 (2003) 127–135.
[22] R. Moriana, F. Vilaplana, S. Karlsson, A. Ribes-Greus, Improved thermo-mechanical properties by the addition of natural fibres in starch-based sustainable biocomposites, Composites A 42 (2011) 30–40.
[23] Y.Z. Wan, H. Luo, F. He, H. Liang, Y. Huang, X.L. Li, Mechanical, moisture absorption, and biodegradation behavior of bacterial cellulose fibre-reinforced start biocomposites, Compos. Sci. Technol. 69 (2009) 1212–1217.
[24] M.J.J. Antal, G. Varhegyi, E. Jakab, Cellulose pyrolysis kinetics: the current state of knowledge, Ind. Eng. Chem. Res. 37 (1998) 1267–1277.
[25] M. Van de Velden, J. Baeyens, A. Brems, R. Dewil, Fundamentals, kinetics and endothermicity of the biomass pyrolysis reaction, Renew. Energy 35 (2010) 232–242.
[26] C. Di Blasi, Modeling chemical and physical processes of wood and biomass pyrolysis, Prog. Energy Combust. Sci. 24 (2008) 47–90.
[27] P. Parasuraman, R. Singh, T. Bolton, S. Omori, R. Francis, Estimation of hardwood lignin concentrations by UV spectroscopy and chlorine demethylation, Bioresources 2 (2007) 459–471.
[28] L. Buessing, J.L. Goldfarb, Energy along interstate-95: pyrolysis kinetics of Floridian cabbage palm (*Sabal palmetto*), J. Anal. Appl. Pyrolysis 96 (2012) 78–85.
[29] M. Brebu, C. Vasile, Thermal degradation of lignin – a review, Cellul. Chem. Technol. 44 (2010) 353–363.
[30] S. Vyazovkin, K. Chrissafis, M.L. Di Lorenzo, N. Koga, M. Pijolat, B. Rodiut, N. Sbirrazzuoli, J.J. Suñol, ICTAC Kinetics Committee recommendations for collecting experimental thermal analysis data for kinetic computations, Thermchim. Acta 590 (2014) 1–23.
[31] A. Aboulkas, K. El harfi, A. El bouadili, Kinetic and mechanism of Tarfaya (Morocco) oil shale and LDPE mixture pyrolysis, J. Mater. Process. Technol. 206 (2008) 16–24.

[32] J. Cai, R. Liu, New distributed activation energy model: numerical solution and application to pyrolysis kinetics of some types of biomass, Bioresour. Technol. 99 (2008) 2795–2799.
[33] Z. Li, C. Liu, Z. Chen, J. Qian, W. Zhao, W. Zhu, Analysis of coals and biomass pyrolysis using the distributed activation energy model, Bioresour. Technol. 100 (2009) 948–952.
[34] T. Mani, P. Murugan, N. Mahinpey, Determination of distributed activation energy model kinetic parameters using annealing optimization method for nonisothermal pyrolysis of lignin, Ind. Eng. Chem. Res. 48 (2009) 1464–1467.
[35] C.P. Please, M.J. McGuinness, D.L.S. McElwain, Approximations to the distributed activation energy model for the pyrolysis of coal, Combust. Flame 133 (2003) 107–117.
[36] T. Sonobe, N. Worasuwannarak, Kinetic analyses of biomass pyrolysis using the distributed activation energy model, Fuel 87 (2008) 414–421.
[37] A. Dawood, K. Miura, Pyrolysis kinetics of γ-irradiated polypropylene, Polym. Degrad. Stabil. 73 (2001) 347–354.
[38] J. Cai, T. Li, R. Liu, A critical study of the Miura–Maki integral method for the estimation of the kinetic parameters of the distributed activation energy model, Bioresour. Technol. 102 (2011) 3894–3899.
[39] C.C. Lakshmanan, N. White, A new distributed activation energy model using Weibull distribution for the representation of complex kinetics, Energy Fuels 8 (1994) 1158–1167.
[40] A. Burnham, R. Braun, Global kinetic analysis of complex materials, Energy Fuels 13 (1999) 1–22.
[41] P.J. Skrdla, Crystallizations, solid-state phase transformations and dissolution behavior explained dispersive kinetic models based on a Maxwell–Boltzmann distribution of activation energies: theory, applications, and practical limitations, J. Phys. Chem. A 113 (2009) 9329–9336.
[42] K. Miura, T. Maki, A simple method for estimating f(E) and k0(E) in the distributed activation energy model, Energy Fuels 12 (1998) 864–869.
[43] J. Chattopadhyay, C. Kim, R. Kim, D. Pak, Thermogravimetric study on pyrolysis of biomass with Cu/Al_2O_3 catalysts, J. Ind. Eng. Chem. 15 (2008) 72–76.
[44] Y.F. Huanga, W.H. Kuanb, P.T. Chiueha, S.L. Lo, Pyrolysis of biomass by thermal analysis–mass spectrometry (TA–MS), Bioresour. Technol. 102 (2011) 3527–3534.
[45] E. Biagini, F. Lippi, L. Petarca, L. Tognotti, Devolatilization rate of biomasses and coal–biomass blends: an experimental investigation, Fuel 81 (2002) 1041–1050.
[46] S. Baumlin, F. Broust, M. Ferrer, N. Meunier, E. Marty, J. Lédé, Continuous self stirred tank reactor: measurement of the cracking kinetics of biomass pyrolysis vapours, Chem. Eng. Sci. 60 (2005) 41–55.
[47] J. Lédé, Cellulose pyrolysis kinetics: an historical review on the existence and role of intermediate active cellulose, J. Anal. Appl. Pyrolysis 94 (2012) 17–32.
[48] G. Várhegyi, M.H. Antal Jr., E. Jakab, P. Szabó, Kinetic modeling of biomass pyrolysis, J. Anal. Appl. Pyrolysis 42 (1997) 73–87.
[49] K. Hashimoto, I. Hasegawa, J. Hayashi, K. Mae, Correlations of kinetic parameters in biomass pyrolysis with solid residue yield and lignin content, Fuel 90 (2011) 104–112.
[50] T.B. Reed, C.D. Cowdery, Heat flux requirements for fast pyrolysis and a new method for generating biomass vapor, in: 193rd National Meeting of the American Chemical Society, April 5–10, Denver, CO, USA, American Chemical Society Division of Petroleum Chemistry, 1987.
[51] R.S. Miller, J. Bellan, A generalized biomass pyrolysis model based on superimposed cellulose, hemicellulose and lignin kinetics, Combust. Sci. Technol. 126 (1997) 97–137.
[52] L. Cabrales, N. Abidi, On the thermal degradation of cellulose in cotton fibers, J. Thermal Anal. Calorim. 102 (2010) 485–491.
[53] L. Gašparovič, J. Labovskŷ, J. Markoš, L. Jelemenský, Calculation of kinetic parameters of the thermal decomposition of wood via the distributed activation energy model (DAME), Chem. Biochem. Eng. 26 (2012) 45–53.
[54] T. Hosoya, H. Kawamoto, S. Saka, Cellulose–hemicellulose and cellulose–lignin interactions in wood pyrolysis at gasification temperature, J. Anal. Appl. Pyrolysis 80 (2007) 118–125.
[55] A. Broido, M. Weinste, Kinetics of solid-phase cellulose pyrolysis, in: H.G. Wiedemann (Ed.), Proceedings of the 3rd International Conference on Thermal Analysis, Birkhauser Verlag, Basel, 1971, pp. 285–296.
[56] A.K. Burnham, R.K. Weese, Kinetics of thermal degradation of explosive binders Viton A, Estane, and Kel-F, Thermochim. Acta 426 (2005) 85–92.
[57] G. Várhegyi, Aims and methods in non-isothermal reaction kinetics, J. Anal. Appl. Pyrolysis 79 (2007) 278–288.